

1 **Changes in morphometric meander parameters identified on the Karoon River,**
2 **Iran, using remote sensing data**

3 **Saleh Yousefi¹, Hamid Reza Pourghasemi*², Janet Hooke³, Oldrich Navartil⁴,**
4 **Anna Kidová⁵**

5 ¹Faculty of Natural Resources and Marine Sciences, Tarbiat Modares University, Emam Reza
6 Street, Noor, P.O.Box: 46417-76489, Iran, Email: saleh.yousefi@modares.ac.ir

7 ²Department of Natural Resources and Environmental Engineering, College of Agriculture,
8 Shiraz University, Shiraz, Iran

9 ³University of Liverpool, Liverpool, UK

10 ⁴ Laboratoire d'étude des Transferts en Hydrologie et Environnement (LTHE) – Université
11 Grenoble 1/IRD, BP 53, 38041-Grenoble Cedex 9, France

12 ⁵Slovak Academy of Sciences, Institute of Geography, Štefánikova 49, 81473Bratislava,
13 Slovakia

14 *Email: hamidreza.pourghasemi@yahoo.com; hr.pourghasemi@shirazu.ac.ir (**Corresponding author**)

15
16 **Abstract**

17 River meander dynamics and mobility are important indicators of environmental
18 change related to climate changes and anthropogenic activities at local and river basin
19 scales. The aim of the present study is to identify morphological changes of the
20 Karoon River in Iran using high accuracy maps and Landsat satellite images by
21 analyses during the time period 1989-2008. In this study, 20 meandering reaches were
22 analyzed over a 128-km-long river reach located in the middle part of the Karoon

23 River, Iran. Morphometric indicators such as: river width (W), meander neck length
24 (L), axis length (A), radius of curvature (R), water flow length (S), and sinuosity of
25 meander (C) were extracted for the identified meanders. The results of a paired t -test
26 showed that river width (W) and meander neck length (L) have significantly changed
27 during the study period (1989-2008), with an increase of +3.5 m for W and a decrease
28 of 274 m for L . Spearman correlation analysis has shown that meander parameter
29 changes are highly correlated to each other. The parameters that do not have
30 significant correlation together are C with W and L , W and L , and L with S and A .
31 During the period of the study, the flow length and river sinuosity decreased for the
32 whole river reach, by 4.77 km and 0.11, respectively. Analysis of land use/ land cover
33 categories (1989 and 2008) using the support vector machine (SVM) and kernel
34 function method served as one of the tools for interpretation of the meander parameter
35 changes. These changes can be attributed not only to LU/LC (riparian vegetation to
36 agriculture area ratio) but also to dam construction in the upstream part of the river
37 that leads to major hydrological regime and sediment transfer alteration. Sediment
38 extraction may also be an important factor.

39 *Keywords:* human impact; land use; meander parameters changes; remote sensing;
40 Karoon River

41 **1. Introduction**

42 River meanders are typical forms of river landscapes that are formed by various
43 factors in fluvial systems (Hooke, 2013). This phenomenon represents
44 hydrogeomorphological forms induced by lateral movement of the river (Dai et al.,

45 2008; Yousefi et al., 2015b). Meanders are among the important features that can
46 change the morphology of floodplains (Lagasse et al., 2004; Güneralp and Rhoads,
47 2009; Güneralp et al., 2012). The behavior of meanders can be associated with major
48 problems for human life, such as destroying residential and farming lands in the
49 floodplain areas. River geomorphic properties are key factors to identifying
50 environmental changes and particularly an association with changes in the river's
51 marginal areas, such as different land cover types in the river sides and drainage basin
52 (Dai et al., 2008). These morphological changes are attributed to changes of water and
53 sediment load regime caused by climate, anthropogenic activities, or land use/land
54 cover changes (Lagasse et al., 2004; Gordon and Meentemeyer, 2006; Cserkés-Nagy
55 et al., 2010)

56 Floodplains and alluvial rivers have been historically and still are one of the most
57 attractive places on Earth for human life and agriculture activities (Allan, 2004; Gordon
58 and Meentemeyer, 2006; Boix-Fayos et al., 2007; James and Lecce, 2013). Land use
59 and land cover (LULC) change is an indirect human impact that could have consequences on
60 river morphology. The LULC change impacts on channel morphology could be considered at
61 catchment or river reach scales (Kondolf et al., 2002; Liébault and Piégay, 2002; Belletti et
62 al., 2016). Changes in the meander parameters can also be attributed to local
63 management activities, as for instance the urbanization expansion, levees, riprap, dam,
64 and road constructions (Nelson et al., 2013). In addition, meanders can naturally
65 evolve and change shape over time even without human intervention (Brice, 1960;
66 Hooke, 1984, 2013).

67 During the last 30 years, different studies on meandering rivers showed that water
68 flow in the meander bend from centrifugal force can cause an intensive increase in
69 water depth and helicoidal flow in the outer arc (Blanckaert, 2003; Frascati and
70 Lanzoni, 2010; Chen and Tang, 2012;). Erosion and sedimentation processes have
71 been observed at the front edge of the meander arcs (Frothingham and Rhoads, 2003;
72 Rhoads et al., 2009; Riley and Rhoads, 2012). Bank erosion along the river will be
73 exacerbated by human intervention in natural conditions and riparian land use changes
74 (Gordon and Meentemeyer, 2006; Rutherford and Price, 2007; Yanan et al., 2011;
75 Yousefi et al., 2015b). Bank erosion and channel migration can occur on different
76 timescales (days, years, decades; Simon and Collison, 2002; Hooke, 2004; Ahmed and
77 Fawzi, 2011; De Rose and Basher, 2011; Michalková et al., 2011). In recent decades,
78 meandering river changes and deformation (narrowing, widening, incision) have been
79 emphasized as of economic, social, and environmental importance (Kondolf, 1994;
80 Allan, 2004; Rinaldi et al., 2005; Boix-Fayos et al., 2007; James and Lecce, 2013;
81 Belletti et al., 2016). In relation to meander parameters and the factors influencing
82 these changes, many studies have been done, especially outside of Iran (Yang et al.,
83 1999; Timár, 2003; Chu et al., 2006; Wolfert and Maas, 2007; Ollero, 2010; Riley and
84 Rhoads, 2012; Ziliani and Surian, 2012; Hooke, 2013; Nabegu, 2014; Liro, 2015;
85 Yousefi et al., 2015b). Various classes and models of meander change have been
86 suggested, but most of these methods are empirical, derived from case studies
87 (Peixoto et al., 2009; Van De Wiel et al., 2011; Güneralp et al., 2012; Fuller et al.,
88 2013; Pirot et al., 2014).

89 This study deals with meander morphology changes of the large Iranian Karoon
90 River between two time horizons (1989 and 2008). Detection of the land use and land
91 cover change during the study period, based on a support vector machine (SVM)
92 algorithm classification with high accuracy, was key for better understanding of its
93 effect on the river morphology. The classification of the styles of meander change
94 (simple or combined) was identified. Land use and land cover (LULC) changes along
95 the buffer zone of the study reach were recorded. The main aims of the present study
96 are (i) spatio-temporal change of the alluvial part of the Karoon River (ii) effects of
97 two main controlling factors (land use and gravel mining) on river geomorphology.

98 **2. Study area**

99 The Karoon River is located in the southwest of Iran; and from a hydro-energy point
100 of view (dams in the upstream zone), it is the most important meandering Iranian
101 river, with the highest discharge, length, and catchment area among all rivers in Iran.
102 The Karoon River total length is about 950 km and the catchment area is about 67,500
103 km², with a population of 3.5 million people living in the catchment. The source of
104 water for the Karoon River is Zagros Mountain with elevation of 4548 m asl, and in
105 the downstream it joins with the Arvanrood River in Khoramshahr City, at an
106 elevation of 12 m asl (Salarijazi, 2012). The Karoon catchment has a large range of
107 elevations and it covers different types of climates. The Zagros Mountains (Aghajari,
108 Mishan, and Bakhtyari) are geologically very heterogeneous with limestone, marly-
109 limestone, marl, shale, sandstone, and conglomerate. The lowland areas include recent
110 alluvial sediments. The long-term mean annual daily discharge at the Ahvaz gauging
111 station over more than three decades (1972-2009) is 504 m³s⁻¹ and maximum annual

112 discharge is $2756 \text{ m}^3\text{s}^{-1}$. Dissolved sediment load is 10 g l^{-1} . In recent decades, many
113 large dams were constructed for water storage, energy production, and irrigation
114 purposes in this area (Salarijazi, 2012).

115 The studied river reach of the Karoon River is 128 km long (Fig. 1). Its upstream
116 part is located close to one of the biggest dams in Iran, namely Gotvand Dam, built in
117 2003. The 180-m-high dam creates a reservoir volume of about 28.5million m^3 . The
118 downstream part of the river reach is located near Shoshtar City. A 3-km buffer area
119 was defined along the study reach to monitor wider spatial changes (49,414 ha). It
120 includes the cities of Shoshtar (187,337 inhabitants) and Gotvand (59,261
121 inhabitants).

122 **3. Methodology**

123 *3.1. Data used*

124 Figure 2 shows the flowchart of the methodology applied for clarifying morphological
125 changes using remote sensed data for measuring bend parameters and amounts of
126 LULC change along the 128-km channel length in the selected study reach. In this
127 study, different Landsat images were used (Table 1). The geometric corrections with a
128 nonparametric polynomial method were applied to the images according to 34 ground
129 control points in stable parts of the vector road and stream layers. On stable sections
130 of channelized river reaches and roads, 29 control points were selected. The total error
131 of corrections was estimated according to root mean standard error (RMSE) and gives
132 0.34 in each pixel (30 m). Because no clouds were present at the time of the survey,
133 no atmospheric correction was applied to the images. In the study reach, high

134 accuracy maps (1:10,000) produced by the Geological Surveys of Iran (GSI) have
135 been used for identification of meander morphometric parameters. One of the most
136 important points in this study is the spatial resolution (30 m) of images used for land
137 use maps; these limits are a source of uncertainty in this study. Recent studies
138 (Gualtieri and Crompton, 1999; Halder et al. 2011) demonstrated that support vector
139 machine performs better than other algorithms to produce land cover maps, especially
140 when a small number of training data are available. Obviously, the use of high-
141 resolution images reduces the uncertainty in research, but accessibility to recent
142 decades of data, freely downloadable, are the main reasons to use Landsat data in the
143 current research. Moreover, many published papers focus on channel morphology
144 changes that used Landsat data which gives us more confidence (Chu et al., 2006;
145 Peixoto et al., 2009; Ahmed and Fawzi, 2011; Thakur et al., 2012; Henshaw et al.,
146 2013). As the river reach in both study dates is very important to geomorphological
147 analysis and to the Landsat data (TM and ETM+) we cannot reach high spatial
148 resolution in the present study; thus, the morphometric parameters have been extracted
149 based on 1:10,000 scale maps.

150 *3.2. Land use mapping in 1989 and 2008 and their change detection*

151 For the method of land use and land cover mapping in the study area, training samples
152 were prepared for each land use/land cover type (riparian vegetation, agriculture,
153 residential, water body, and range land) using field surveys and a global positioning
154 system (GPS). The training samples were divided into two parts based on a random
155 partition algorithm (Table 2); one part for use in image classification, and a second
156 class was used to evaluate the classification accuracy according to Perumal and

157 Bhaskaran (2010) and Srivastava et al. (2012). In order to obtain a robust set of
158 training samples, especially for the first image (1989), the questionnaire responses to
159 the question 'what was the land use type of your lands in 1989?' from 118 local native
160 people were used (100 farmers and 18 persons that live in Shoshtar and Gotvand
161 cities). For the land use/land cover map of the study area the support vector machine
162 (SVM) algorithm was used, and the kernel function method was developed for each
163 image. The radial basis function (RBF) was used as the kernel function; and λ in the
164 kernel function represents a value of 0.167, and the value of the penalty parameter
165 achieved 250. A pyramid level was automatically selected as 100 in ENVI 4.7
166 software (Yousefi et al., 2011, 2015a). In this study, detection of the land use and land
167 cover changes between 1989 and 2008 were cross-matched and compared using ENVI
168 4.7 software where the post-classification method based on classified images for both
169 dates was applied (Xu and Gong, 2007; Srivastava et al., 2009, 2012; Yousefi et al.,
170 2011).

171 *3.3. Meander parameters*

172 For considering meander parameters, channel centerlines and bank lines of the
173 study river reach were digitized and divided into 20 meander loops. Meander loop
174 changes have been identified according to Hooke's (1984, 2013) models of meander
175 changes. In this model the meander changes have been classified based on visual and
176 spatial changes. In the study simple or combined types of meander changes
177 (translation, rotation, extension, expansion, cutoff, redevelopment, lateral movement,
178 irregular changes) are presented (Fig. 3B).

179 The specific meander parameters represent axis length (A), meander neck length (L),
180 river width (W), radius of curvature (R), water flow length (S), and sinuosity (C ; Fig. 3A).
181 Axis length is the longest distance between the internal arc and the meander neck. Meander
182 neck is the lowest distance between two meander loops. Water flow length is the length of
183 water between two meander apices. Radius of curvature is the radius of the maximum
184 interior circle in a meander loop, river width (W) is an average of five cross sections
185 (the lowest distances between river banks) in the meander curve (Hooke, 2013).
186 Sinuosity (C) was calculated using the following equation:

$$187 \quad (C = S/L) \quad (1)$$

188 Morphometric parameters for all meander loops in 1989 and 2008 were measured by
189 measurement tools in ArcGIS 10.2. and AUTOCAD 2009.

190 The statistical analysis of paired sample T -tests and Pearson correlations to study
191 the variation of meander parameters and their correlation between 1989 and 2008 was
192 used as the final step.

193 **4. Results**

194 The results of two main types of analysis are presented: first the land use and
195 land cover changes in the buffer zone of the study river reach; and second, the detailed
196 changes of meander parameters between two dates.

198 *4.1. LULC changes*

199 The land use and land cover maps in 1989 and 2008 were prepared using the
200 SVM algorithm and kernel function method (Fig. 4). The overall accuracy and K

201 coefficient of produced LULC maps were calculated and presented in Table 3. The
202 classification accuracy of the LULC map created for 1989 with overall accuracy of
203 88.18% and K coefficient of 0.7879 is lower than the LULC map created for 2008
204 with overall accuracy of 94.51% and K coefficient of 0.8937. The results showed that
205 the areas of water body, riparian vegetation, and rangeland have decreased over the
206 study period (Fig. 5). In contrast, agriculture and residential land cover types have
207 increased. However, the LULC maps with detected changes (Fig. 6) showed that 24%
208 of the study area has been changed (120 km²), and water body and riparian vegetation
209 areas had the highest changes in the study area, with 54% and 52%, respectively
210 (Table 4).

211 *4.2. Meander parameter changes and statistical analysis*

212 Channel centerlines of the study reach were digitized and 20 meander loops
213 were selected for two time horizons (Fig. 7). Morphometric parameters for all
214 meander loops in 1989 and 2008 were measured, and the morphological change of
215 meander loops were calculated (Table 5). Mean values of the river width between
216 1989 and 2008 indicate a decreasing trend of the river width. On the contrary, the
217 sinuosity (C) during the two decades increased. Results of meander morphological
218 variables show that the standard deviation (SD) of R and S in 1989 is higher than in
219 2008. On the other hand, the SD of W , A , L , and C in 2008 is higher than 1989. These
220 results show that the variability of river width (W) and water flow length (S) among 20
221 study meanders in 1989 are more than the 2008 values.

222 Results of meander morphological change show that in the study reach three
223 types of meander change (simple, double, and triple). Several meander (number 4, 5,

224 7, 15, 18, 20) loops with the greatest morphological changes represent combinations
225 of double and triple types of change (Fig. 8). In addition, in three meander loops
226 cutoff and redevelopment of meanders have been observed (meanders 9, 10, and 11);
227 all of these meanders are located between two sand extraction mines. Besides, more
228 than half (11) of all studied meanders were assigned simple change represented by
229 translation, rotation, lateral movement, expansion, or irregular changes.

230 According to paired samples *T*-test (Table 6) for studying the variation of
231 meander parameters, a significant change within 5% confidence level between the two
232 dates for the meander neck length (*L*) and the meander width (*W*). In contrast, no
233 significant difference was observed for radius of curvature (*R*), water flow length (*S*),
234 sinuosity (*C*), and meander axis length (*A*) between the mentioned dates.

235 The results of the Pearson correlation between meander parameter changes are
236 given in Table 7. Table 7 shows that a significant correlation between sinuosity
237 changes (*C*) and radius of curvature (*R*), water flow length (*S*), and axis length (*L*)
238 changes at confidence level of 5%, 1%, and 1%, respectively. Significant correlation
239 was also found between change in the radius of curvature (*R*) with water flow length
240 (*L*), axis length (*A*), meander neck length, and river width changes at a significance
241 level of 5%, 1%, 1%, and 1%, respectively. In addition, a significant correlation
242 between changes in the river width (*W*), water flow length (*L*), and axis length (*A*)
243 changes at a confidence level of 1%. Also water flow length (*L*) has a significant
244 correlation at the 1% level with axis length (*A*) of the meander (Table 7).

247

5. Discussion

248

249

250

251

252

253

254

255

256

257

258

259

260

261

Morphological changes in river systems relate together like a chain (Lagasse et al., 2004). Recorded changes in radius of curvature (R) caused by enlargement of the internal arc led to an increase of water flow length (S) and enlargement of meander neck length (L). The axis length (A) increased by this process, too. According to the sinuosity coefficient (C), increasing values of morphometric parameters (S and L) apparently increased the sinuosity of meander in 2008. The river width (W) changes are inversely related to the changes of water flow length (S) and axis length (A) of the meander. The axis length of meanders represents the transverse fluctuations. Indeed, the consequence of factors such as geological type of the river bed, hydrological conditions of the river, and alteration of the river bed. If meander neck length (L) remains constant over time, the radius of curvature (R) will decrease and sinuosity (C) of meanders increases (Crosato, 2008; Heo et al., 2009). In general, results show a direct relationship between radius of curvature changes and changes of sinuosity, meander neck length, water flow length, and axis length of meander (Table 7).

262

263

264

265

266

267

268

In the study area, the riparian vegetation, water body, and range land type areas have decreased by 262, 351, and 214 ha, respectively. On the other hand, agricultural and residential areas increased by 304 ha and 522 ha, respectively. Range lands, riparian vegetation, and floodplain areas are the property of the government institution of the National lands in Iran. Because of the low levels of land protection in National lands, the stakeholders every year pushed to change the types of these lands to types like residential or agricultural because of financial attractiveness.

269 In parts of the river where agriculture comes near to the river banks, river width (W)
270 was reduced (Fig. 9). According to Yanan et al. (2011), when river width is reducing
271 and a cutoff occurs, the river slope is increasing, i.e., the same amount of water
272 discharge is forced to flow down the river more quickly in the smaller, steeper, and
273 narrowed section. Increase of water velocity caused an increase of stream power and
274 greater bank erosion that resulted in an increase in water flow length (S) and axis
275 length (A) of meanders in our studied reach.

276 According to field surveys and assessment of land use maps in 1989 and 2008, the
277 study area, particularly in the river margins (i.e., 3-km buffer zone along the river
278 length) has been interrupted by human activities such as irrigation channels,
279 residential land sprawl, and sand mining. Human impact as a crucial factor of river
280 morphology changes is documented in several papers (Liébault and Piégay, 2002;
281 Zaimes et al., 2004; James and Lecce, 2013; Yousefi et al., 2015; Belletti et al., 2016
282). This activity was observed with greater intensity in meanders 8 to 13 (Fig. 9), where
283 destruction of riparian area and conversion to agricultural land has been most
284 observed. The high quality of the soils in the upstream part and particularly the
285 alluvial banks and the riparian covers are the main reasons that encourage the local
286 people that live in the marginal area to plough the land and change the land to farming
287 area near the river banks. According to Güneralp et al. (2012), plowing the land and
288 destroying the natural vegetation of the river cause soil loss and therefore degradation
289 of the meander outer arc. Riparian vegetation is one of the most important factors that
290 controls bank erosion as the main process of river migration (Timár, 2003; Cabezas et
291 al., 2008; Ollero, 2010; Engel and Rhoads, 2012). Ahmed and Fawzi (2011a) in a

292 study of the Nile River reported that in agricultural land bank erosion and river
293 widening is more than in riparian vegetation lands, similar to our results.

294 Sand extraction on the river floodplain to obtain sand for urban and dam construction,
295 changes the waterway, soil stability, and cohesion by removing organic matter.
296 Removal of cohesive components such as clay and organic material (wood, grass, and
297 roots) makes the soil more erodible (Kondolf, 1994; Rinaldi et al., 2005; Cserkés-
298 Nagy et al., 2010; Martín-Vide et al., 2010; Gutierrez et al., 2014; Smith et al., 2016).
299 In the study site four active sand mining factories. Meanders that are near the
300 extraction sites have anabranch shapes and high changes as a consequence of river bed
301 disturbance (Latapie et al., 2014). Meander number 20 is affected by mines where
302 sand was extracted for dam construction and meanders 9, 10, and 11 are affected by
303 mines that were worked for building construction. According to the meander change
304 classification method, meander number 20 has the triple combination type of
305 extension, translation, and rotation processes; while in meanders number 9, 10, and 11
306 the cutoff process has occurred and then meanders have redeveloped. Dai et al. (2008)
307 have reported the effect of uncontrolled sand extraction in the Pearl River in China
308 over the last two decades; the abnormal changes in meanders near the sand mines
309 demonstrated in this study are similar to those results. Brunier et al. (2014) also
310 mentioned the effects of sand extraction on increasing flow paths in the Mekong delta
311 in Vietnam.

312 The Gotvand Dam is one of the largest dams in Iran and is the last downstream dam
313 on the Karoon River. Gotvand Dam has some impact on Karoon discharge and
314 sediment load as, before dam construction, the average daily discharge (1972-2002)

315 was $534 \text{ m}^3\text{s}^{-1}$, but after the dam was constructed the average daily discharge (2003-
316 2009) decreased to $490 \text{ m}^3\text{s}^{-1}$. Average daily suspended sediment load for before and
317 after dam construction were 16.36 and 9.12 g l^{-1} , respectively. Results of meander
318 change classifications show that most of the study meanders have two types of
319 change, simple and double (16 meanders), and in most of them the meander has a
320 simple combination of change in its form; this could be because of the controlling role
321 of Gotvand Dam. In addition, in the study area three cutoffs located between two
322 mining sites appeared during the study period. Gravel mining in some cases changes
323 the structure and form of the river bed and consequently water flow changes the
324 direction of the channel to more erodible sides (James, 1991; Liébault and Piégay,
325 2002; Batalla, 2003; Rinaldi et al., 2005; Martín-Vide et al., 2010; Belletti et al., 2016
326). We suggest that further studies can be done on the rate of changes and monitoring
327 and evaluation in the area.

329 **6. Conclusion**

330 An understanding of fluvial system response over recent decades is essential
331 knowledge to assess and predict effects of human disturbances on watershed areas and
332 fluvial systems (Latapie et al., 2014). The main aim of the current study was to
333 investigate and identify morphological changes in a part of the Karoon River over the
334 period 1989 to 2008 and the possible effects of land use on morphological changes
335 using remote sensing data. During the study, the river flow length and river sinuosity
336 decreased for the that river reach by 4.77 km and 0.11 , respectively. This decrease is
337 mainly because of cutoffs in three meanders which are all located between two sand

338 extraction sites. Gravel mining has direct effects on river morphology; in mining sites
339 by extracting sand and gravel, the flow of the river and the power of the water always
340 find the easier way to flow. Land use maps were prepared using the SVM algorithm;
341 and results of land use change detection showed that during two decades, 1928 ha of
342 water body and riparian vegetation were converted to agricultural lands. Gotvand Dam
343 has a controlling role on the sediment load in the study area; also this dam decreased
344 the average daily discharge of downstream by about $44 \text{ m}^3\text{s}^{-1}$. By decreasing flow
345 discharge, the power of flow decreased and high intensity floods were controlled by
346 the constructed dams; and as a consequence, the river form has adjusted in most of the
347 meander. However, in meanders that have been affected by sand extraction, this is not
348 true (Gordon and Meentemeyer, 2006; Dai et al., 2008; Lorenz et al., 2009; Ma et al.,
349 2012; Csiki and Rhoads, 2014; Grenfell et al., 2014; Yousefi et al., 2015b). Finally we
350 can say that sand mining has a significant role in decreasing the flow length by
351 increasing the probability of cutoff events; dam building (discharge controlling) and
352 land use change (removal of the riparian vegetation) have an important role in
353 decreasing channel width in the study reach of the Karoon River.

354 Exploration of the meander parameters can help to predict future trends in river
355 morphology and meander evolution. Understanding the changing meander parameters
356 could help to achieve better river management and mitigation of the damages
357 associated with these changes.

361 **Acknowledgement**

362 The authors would like to thank two anonymous reviewers for their helpful comments on the
363 primary version of the manuscript. Also, we are to extremely grateful to Prof. Dr. Richard A.
364 Marston (Editor, *Geomorphology*) for adding positive comments.
365

366 **References**

367 Ahmed, A. a., Fawzi, A., 2011. Meandering and bank erosion of the River Nile and its
368 environmental impact on the area between Sohag and El-Minia, Egypt. *Arabian*
369 *Journal of Geosciences* 4, 1–11.

370 Allan, J.D., 2004. Landscapes and riverscapes: the influence of land use on stream
371 ecosystems. *Annual review of ecology, evolution, and systematics. Annual*
372 *Review of Ecology Evolution and Systematics* 35, 257-284.

373 Batalla, R.J., 2003. Sediment deficit in rivers caused by dams and instream gravel
374 mining: A review with examples from NE Spain. *Cuaternario y geomorfología:*
375 *Revista de la Sociedad Española de Geomorfología y Asociación Española para*
376 *el Estudio del Cuaternario* 17(3), 79-91.

377 Belletti, B., Nardi, L. and Rinaldi, M., 2016. Diagnosing problems induced by past
378 gravel mining and other disturbances in Southern European rivers: the Magra
379 River, Italy. *Aquatic Sciences* 78(1), 107-119.

380 Blanckaert, K., 2003. Nonlinear modeling of mean flow redistribution in curved open
381 channels. *Water Resources Resarch* 39, 1–14.

382 Boix-Fayos, C., Barberá, G., López-Bermúdez, F. and Castillo, V., 2007. Effects of
383 check dams, reforestation and land-use changes on river channel morphology:

384 Case study of the Rogativa catchment (Murcia, Spain). *Geomorphology* 91(1),
385 103-123.

386 Brice, J.C., 1960. Index for description of channel braiding. *Geological Society of*
387 *America Bulletin* 71, 1833.

388 Brunier, G., Anthony, E.J., Goichot, M., Provansal, M., Dussouillez, P., 2014. Recent
389 morphological changes in the Mekong and Bassac river channels, Mekong delta:
390 The marked impact of river-bed mining and implications for delta destabilisation.
391 *Geomorphology* 224, 177–191.

392 Cabezas, a., Comin, F. a., Begueria, S., Trabucchi, M., 2008. Hydrologic and land-
393 use change influence landscape diversity in the Ebro River (NE Spain).
394 *Hydrological Earth System Sciences and Discussion* 5, 2759–2789.

395 Camporeale, C., Ridolfi, L., 2010. Interplay among river meandering, discharge
396 stochasticity and riparian vegetation. *Journal of Hydrology* 382, 138–144.

397 Chen, D., Tang, C., 2012. Evaluating secondary flows in the evolution of sine-
398 generated meanders. *Geomorphology* 163-164, 37–44.

399 Chu, Z.X., Sun, X.G., Zhai, S.K., Xu, K.H., 2006. Changing pattern of
400 accretion/erosion of the modern Yellow River (Huanghe) subaerial delta, China:
401 Based on remote sensing images. *Marine Geology* 227, 13–30.

402 Constantine, C.R., Dunne, T., Hanson, G.J., 2009. Examining the physical meaning of
403 the bank erosion coefficient used in meander migration modeling.
404 *Geomorphology* 106, 242–252.

405 Crosato, A., 2008. Analysis and modelling of river meandering. IOS Press,

406 Amsterdam, 251 pp.

407 Cserkész-Nagy, Á., Tóth, T., Vajk, Ö., Sztanó, O., 2010. Erosional scours and
408 meander development in response to river engineering: Middle Tisza region,
409 Hungary. *Proceedings of the Geologists' Association* 121, 238–247.

410 Csiki, S.J.C., Rhoads, B.L., 2014. Influence of four run-of-river dams on channel
411 morphology and sediment characteristics in Illinois, USA. *Geomorphology* 206,
412 215–229.

413 Dai, S.B., Yang, S.L., Cai, a. M., 2008. Impacts of dams on the sediment flux of the
414 Pearl River, southern China. *Catena* 76, 36–43.

415 De Rose, R.C., Basher, L.R., 2011. Measurement of river bank and cliff erosion from
416 sequential LIDAR and historical aerial photography. *Geomorphology* 126, 132–
417 147.

418 Engel, F.L., Rhoads, B.L., 2012. Interaction among mean flow, turbulence, bed
419 morphology, bank failures and channel planform in an evolving compound
420 meander loop. *Geomorphology* 163-164, 70–83.

421 Frascati, A., Lanzoni, S., 2010. Long-term river meandering as a part of chaotic
422 dynamics? A contribution from mathematical modelling. *Earth Surface Process
423 and Landforms* 35, 791–802.

424 Frothingham, K.M., Rhoads, B.L., 2003. Three-dimensional flow structure and
425 channel change in an asymmetrical compound meander loop, Embarras River,
426 Illinois. *Earth Surface Process and Landforms* 28, 625–644.

427 Fuller, I.C., Reid, H.E., Brierley, G.J., 2013. *Methods in Geomorphology:*

428 Investigating River Channel Form, Treatise on Geomorphology. Elsevier Ltd.

429 Giriraj, A., Irfan-Ullah, M., Murthy, M.S.R., Beierkuhnlein, C., 2008. Modelling
430 spatial and temporal forest cover change patterns (1973-2020): A case study from
431 South Western Ghats (India). *Sensors* 8, 6132–6153.

432 Gordon, E., Meentemeyer, R.K., 2006. Effects of dam operation and land use on
433 stream channel morphology and riparian vegetation. *Geomorphology* 82, 412–
434 429.

435 Grenfell, M.C., Nicholas, a. P., Aalto, R., 2014. Mediative adjustment of river
436 dynamics: The role of chute channels in tropical sand-bed meandering rivers.
437 *Sedimentary Geology* 301, 93–106.

438 Güneralp, I., Rhoads, B.L., 2009. Empirical analysis of the planform curvature-
439 migration relation of meandering rivers. *Water Resources Research* 45, 1–15.

440 Güneralp, I., Abad, J.D., Zolezzi, G., Hooke, J., 2012. Advances and challenges in
441 meandering channels research. *Geomorphology* 163-164, 1–9.

442 Gutierrez, R.R., Abad, J.D., Choi, M., Montoro, H., 2014. Characterization of
443 confluences in free meandering rivers of the Amazon basin. *Geomorphology* 220,
444 1–14.

445 Henshaw, A.J., Gurnell, A.M., Bertoldi, W., Drake, N. a., 2013. An assessment of the
446 degree to which Landsat TM data can support the assessment of fluvial dynamics,
447 as revealed by changes in vegetation extent and channel position, along a large
448 river. *Geomorphology* 202, 74–85.

449 Heo, J., Duc, T.A., Cho, H.S., Choi, S.U., 2009. Characterization and prediction of

450 meandering channel migration in the GIS environment: A case study of the
451 Sabine River in the USA. *Environmental Monitoring and Assessment* 152, 155–
452 165.

453 Hooke, J., 1984. Changes in river meanders – a review of techniques and results of
454 analyses. *Progress in Physical Geography* 8, 473–508.

455 Hooke, J.M., 2004. Cutoffs galore!: Occurrence and causes of multiple cutoffs on a
456 meandering river. *Geomorphology* 61, 225–238.

457 Hooke, J. M., 2013. River Meandering. In E. Wohl, & J. Schroder (Eds.), *Treatise on*
458 *Geomorphology* 9, 260-288

459 Howard, A.D., 2009. How to make a meandering river. *Proceeding of the National*
460 *Academy of Sciences of the United States of America* 106, 17245–17246.

461 James, L. Lecce, S., 2013. Impacts of land-use and land-cover change on river
462 systems. Shroder, Jr., J. (Ed. in chief), Wohl, E.(Eds.), *Treatise on*
463 *Geomorphology* 9, 768-793.

464 James, L.A., 1991. Incision and morphologic evolution of an alluvial channel
465 recovering from hydraulic mining sediment. *Geological Society of America*
466 *Bulletin* 103(6), 723-736.

467 Kondolf, G.M., 1994. Geomorphic and environmental effects of instream gravel
468 mining. *Landscape and Urban Planning* 28(2), 225-243.

469 Kondolf, G., Piégay, H. and Landon, N., 2002. Channel response to increased and
470 decreased bedload supply from land use change: contrasts between two
471 catchments. *Geomorphology* 45(1), 35-51.

472 Lagasse, P.F., Zevenbergen, L.W., Spitz, W.J., Thorne, C.R., Associates, A., Collins,
473 F., 2004. Methodology for Predicting Channel Migration, Rivers. NCHRP Web-
474 Only Document 67 (Project 24-16)

475 Latapie, a., Camenen, B., Rodrigues, S., Paquier, a., Bouchard, J.P., Moatar, F.,
476 2014. Assessing channel response of a long river influenced by human
477 disturbance. *Catena* 121, 1–12.

478 Liébault, F. and Piégay, H., 2002. Causes of 20th century channel narrowing in
479 mountain and piedmont rivers of southeastern France. *Earth Surface Processes*
480 *and Landforms* 27(4), 425-444.

481 Liro, M., 2015. Gravel-bed channel changes upstream of a reservoir: The case of the
482 Dunajec River upstream of the Czorsztyn Reservoir, southern Poland.
483 *Geomorphology* 228, 694–702.

484 Lofthouse, C., Robert, A., 2008. Riffle-pool sequences and meander morphology.
485 *Geomorphology* 99, 214–223.

486 Lorenz, A.W., Jähnig, S.C., Hering, D., 2009. Re-meandering german lowland
487 streams: Qualitative and quantitative effects of restoration measures on
488 hydromorphology and macroinvertebrates. *Environmental Management* 44, 745–
489 754.

490 Ma, Y., Huang, H.Q., Nanson, G.C., Li, Y., Yao, W., 2012. Channel adjustments in
491 response to the operation of large dams: The upper reach of the lower Yellow
492 River. *Geomorphology* 147-148, 35–48.

493 Martín-Vide, J., Ferrer-Boix, C. and Ollero, A., 2010. Incision due to gravel mining:

494 Modeling a case study from the Gállego River, Spain. *Geomorphology* 117(3),
495 261-271.

496 Michalková, M., Piégay, H., Kondolf, G.M. and Greco, S.E., 2011. Lateral erosion of
497 the Sacramento River, California (1942-1999), and responses of channel and
498 floodplain lake to human influences. *Earth Surface Processes and Landforms*
499 36(2), 257-272.

500 Nabegu, A.B., 2014. Impact of Urbanization on Channel Morphology: Some
501 Comments. *IOSR Journal of Environmental Science, Toxicology and Food*
502 *Technology (IOSR-JESTFT)* 8, 40–45.

503 Nardi, L., Rinaldi, M., Solari, L., 2012. An experimental investigation on mass
504 failures occurring in a riverbank composed of sandy gravel. *Geomorphology* 163-
505 164, 56–69.

506 Nelson, N.C., Erwin, S.O., Schmidt, J.C., 2013. Spatial and temporal patterns in
507 channel change on the Snake River downstream from Jackson Lake dam,
508 Wyoming. *Geomorphology* 200, 132–142.

509 Ollero, A., 2010. Channel changes and floodplain management in the meandering
510 middle Ebro River, Spain. *Geomorphology* 117, 247–260.

511 Peixoto, J.M. a, Nelson, B.W., Wittmann, F., 2009. Spatial and temporal dynamics of
512 river channel migration and vegetation in central Amazonian white-water
513 floodplains by remote-sensing techniques. *Remote Sensing and Environment* 113,
514 2258–2266.

515 Perucca, E., Camporeale, C., Ridolfi, L., 2006. Influence of river meandering

516 dynamics on riparian vegetation pattern formation. *Journal of Geophysical*
517 *Researche Biogeosciences* 111, 1–9.

518 Perumal, K., Bhaskaran, R., 2010. Supervised classification performance of
519 multispectral images. *Journal of Computing* 2, 124–129.

520 Pirot, G., Straubhaar, J., Renard, P., 2014. Simulation of braided river elevation model
521 time series with multiple-point statistics. *Geomorphology* 214, 148–156.

522 Posner, A.J., Duan, J.G., 2012. Simulating river meandering processes using
523 stochastic bank erosion coefficient. *Geomorphology* 163-164, 26–36.

524 Rhoads, B.L., Riley, J.D., Mayer, D.R., 2009. Response of bed morphology and bed
525 material texture to hydrological conditions at an asymmetrical stream confluence.
526 *Geomorphology* 109, 161–173.

527 Riley, J.D., Rhoads, B.L., 2012. Flow structure and channel morphology at a natural
528 confluent meander bend. *Geomorphology* 163-164, 84–98.

529 Rinaldi, M., Wyżga, B. and Surian, N., 2005. Sediment mining in alluvial channels:
530 physical effects and management perspectives. *River Research and Applications*
531 21(7), 805-828.

532 Rusnák, M., Lehotský, M., 2013. Time-focused investigation of river channel
533 morphological changes due to extreme floods. *Zeitschrift für Geomorphologie* 58,
534 2, 251-266.

535 Rutherford, I., Price, P., 2007. Management on Stream Erosion, in: *The Influence of*
536 *Riparian Managment on Stream Erosion*. Land & Water Australia, Canberra, pp.
537 86–116.

538 Salarijazi, M., 2012. Trend and change-point detection for the annual stream-flow
539 series of the Karun River at the Ahvaz hydrometric station. *African Journal of*
540 *Agricultural Research* 7, 4540–4552.

541 Seker, D.Z., Kaya, S., Musaoglu, N., Kabdasli, S., Yuasa, A., Duran, Z., 2005.
542 Investigation of meandering in Filyos River by means of satellite sensor data.
543 *Hydrological Processes* 19, 1497–1508.

544 Simon, A. and Collison, A.J., 2002. Quantifying the mechanical and hydrologic
545 effects of riparian vegetation on streambank stability. *Earth Surface Processes*
546 *and Landforms* 27(5), 527-546.

547 Smith, C. Bowie, M.H., Hahner, J.L., Boyer, S., Kim, H.T., Abbott, M., Rhodes, S.,
548 Sharp, D., Dickinson, N., 2016. Punakaiki Coastal Restoration Project: A case
549 study for a consultative and multidisciplinary approach in selecting indicators of
550 restoration success for a sand mining closure site, West Coast, New Zealand.
551 *Catena* 136, 91-103.

552 Solín, Ľ., Feranec, J., Nováček, J., 2011. Land cover changes in small catchments in
553 Slovakia during 1990-2006 and their effects on frequency of flood events.
554 *Natural Hazards* 56, 195-214.

555 Srivastava, P.K., Majumdar, T.J., Bhattacharya, A.K., 2009. Surface temperature
556 estimation in Singhbhum Shear Zone of India using Landsat-7 ETM + thermal
557 infrared data. *Advances in Space Research* 43, 1563–1574.

558 Srivastava, P.K., Han, D., Rico-Ramirez, M. a., Bray, M., Islam, T., 2012. Selection
559 of classification techniques for land use/land cover change investigation.

560 Advances in Space Research 50, 1250–1265.

561 Thakur, P.K., Laha, C., Aggarwal, S.P., 2012. River bank erosion hazard study of
562 river Ganga, upstream of Farakka barrage using remote sensing and GIS. *Natural*
563 *Hazards* 61, 967–987.

564 Timár, G., 2003. Controls on channel sinuosity changes: A case study of the Tisza
565 River, the Great Hungarian Plain. *Quaternary Science Reviews* 22, 2199–2207.

566 Van De Wiel, M.J., Coulthard, T.J., Macklin, M.G., Lewin, J., 2011. Modelling the
567 response of river systems to environmental change: Progress, problems and
568 prospects for palaeo-environmental reconstructions. *Earth Science Review* 104,
569 167–185.

570 Wolfert, H.P., Maas, G.J., 2007. Downstream changes of meandering styles in the
571 lower reaches of the River Vecht, the Netherlands. *Geologie en Mijnbouw* 86,
572 257–271.

573 Xu, B., Gong, P., 2007. Land-use / Land-cover Classification with Multispectral and
574 Hyperspectral EO-1 Data 73, 955–965.

575 Yanan, L., Yuliang, Q., Yue, Z., 2011. Dynamic Monitoring and Driving Force
576 Analysis on Rivers and Lakes in Zhuhai City Using Remote Sensing
577 Technologies. *Procedia Environmental Sciences* 10, 2677–2683.

578 Yang, X., Damen, M.C., van Zuidam, R. a, 1999. Satellite remote sensing and GIS
579 for the analysis of channel migration changes in the active Yellow River Delta,
580 China. *International Journal of Applied Earth Observation and Geoinformation* 1,
581 146–157.

582 Yousefi, S., Moradi, H.R., Hosseini, S.H., Mirzaee, S., 2011. Land use change
583 detection using Landsat TM and ETM+ satellite image over Marivan. Journal of
584 RS and GIS for Natural Resources (Journal of Applied RS and GIS Techniques in
585 Natural Resources Science) 2, 97–105.

586 Yousefi, S., Khatami, R., Mountrakis, G., Mirzaee, S., Pourghasemi, H.R., Tazeh, M.,
587 2015a. Accuracy assessment of land cover / land use classifiers in dry and humid
588 areas of Iran. Environmental Monitoring and Assessment 187 (10):
589 641.doi:10.1007/s10661-015-4847-1

590 Yousefi, S., Moradi, H.R., Tevari, A., Vafakhah, M., 2015b. Monitoring of fluvial
591 systems using RS and GIS (Case study: Talar River, Iran). Journal of Selçuk
592 University Natural and Applied Science 4, 60–72.

593 Zaimes, G., Schultz, R., Isenhardt, T., 2004. Stream bank erosion adjacent to riparian
594 forest buffers, row-crop fields, and continuously-grazed pastures along Bear
595 Creek in central Iowa. Journal of Soil Water Conservation 59, 19–27.

596 Zhang, B., Ai, N., Huang, Z., Yi, C., Qin, F., 2008. Meanders of the Jialing River in
597 China: Morphology and formation. Chinese Science Bulletin 53, 267–281.

598 Zhang, Y., Wang, P., Wu, B., Hou, S., 2015. An experimental study of fluvial
599 processes at asymmetrical river confluences with hyperconcentrated tributary
600 flows. Geomorphology 230, 26–36.

601 Ziliani, L., Surian, N., 2012. Evolutionary trajectory of channel morphology and
602 controlling factors in a large gravel-bed river. Geomorphology 173-174, 104–
603 117.

604

605

606

607

608

609

610

611

612

613

614

615

616

617

618

619

620

621

622

Figures caption

623 **Fig. 1.** Location of study area in Khozestan Province, Iran.

624 **Fig. 2.** Flow chart of the used methodology based on geometric correction of remote sensed
625 data, land use/land cover, and river features evaluation (meander parameters).

626 **Fig. 3.** (A) Morphometric parameters of study meanders: axis length (A), meander neck
627 length (L), river width (W), radius curvature (R), water flow length (S). (B) Model of meander
628 change based on Hooke (1984).

629 **Fig. 4.** Land use maps in 1989 and 2008.

630 **Fig. 5.** Areal changes in five land use/land cover types during the study period.

631 **Fig. 6.** Detection of land use/land cover changes during the study period.

632 **Fig. 7.** Study meanders and centerlines of the study river reach with marked areas of sand
633 mining.

634 **Fig. 8.** Morphological change of the most variable meanders in the study river reach.

635 **Fig. 9.** Morphological change of the most variable meanders and land use/land cover change.
636

637

638

639

640

641

Table 1

642

Data used in the study area

Data	Date	Scale/resolution	Provider	Discharge $\text{m}^3 \text{s}^{-1}$
TM	23/May/1989	30*30 meters	USGS	569
ETM+	5/June/2008	30*30 meters	USGS	325
Topography map	25/March/2001	1:25,000	National Cartographic Center of Iran (NCC)	550
Geology map	10/March/2008	1:100,000	Geological Surveys of Iran (GSI)	413
Active channel plan	12/June/1989	1:10000	Geological Surveys of Iran (GSI)	518
Active channel plan	12/July/2008	1:10000	Geological Surveys of Iran (GSI)	301

643

644

645

646

647

648

649

650

651

652

653

654

655

Table 2
Training sample characteristics

Land use/land cover types	Training sample				
	Number of training samples	Classification (ha)	Evaluation (ha)	Classification (pixels)	Evaluation (pixels)
Riparian vegetation	86	41.48	17.26	460	192
Agriculture	207	469.4	137.67	5215	1528
Residential	48	6.16	1.87	68	20
Water body	39	6.3	1.7	70	18
Range land	112	145.7	40.3	1618	447

656

657

658

659

660

661

662

663

664

665

666

667

668

669

670

671

672

673

674

675

676

677
678
679

680

681
682
683
684
685
686
687
688
689
690
691
692
693
694
695
696
697
698
699
700
701
702

Table 3

Coefficient classification accuracy of the produced land use/land cover maps based on using ground control points

Year	Overall accuracy (%)	Kappa coefficient
1989	88.18	0.7876
2008	94.51	0.8937

703

Table 4

704

Detection of the land use and land cover changes during the study period

Land use/land cover changes between 1989 and 2008	Area (ha)	Percent
Agriculture no change	26314.8	82.64
Agriculture to Range land	3375.1	10.6
Agriculture to Residential	837.2	2.63
Agriculture to Riparian vegetation	837.67	2.63
Agriculture to Water body	479.1	1.5
Range land no change	7107.9	65.39
Range land to Agriculture	3477.2	31.99
Range land to Residential	284.4	2.62
Residential no Change	1570.9	96.05
Residential to Water body	64.6	3.95
Riparian vegetation no change	1448.4	47.9
Riparian vegetation to Agriculture	1334.04	44.12
Riparian vegetation to Residential	35.9	1.19
Riparian vegetation to Water body	205.2	6.79
Water body no change	920.8	45.12
Water body to Agriculture	594.6	29.13
Water body to Residential	124.9	6.12
Water body to Riparian vegetation	400.7	19.63

705

706

707

708

709

710

711

712

713

714

715

716

717

718

719

720

721
722
723
724
725

Table 5

Meander parameters as river width (*W*), radius curvature (*R*), axis length (*A*), meander neck length (*L*), water flow length (*S*), and sinuosity (*C*) measured on the study river reach in two time horizons (1989 and 2008) and morphological change of meander loops (SD – standard deviation)

Number	1989						2008						Morphological change (1989-2008)	
	W (km)	R (km)	A (km)	L (km)	S (km)	C	W(km)	R (km)	A (km)	L (km)	S (km)	C	Type of change	Description
1	0.253	1.6	4.13	5.44	10.31	1.89	0.173	1.85	3.94	5.1	10.42	2.04	Simple	Translation
2	0.217	1.41	3.2	5.4	8.31	1.54	0.183	1.23	3.17	5.58	8.51	1.53	Simple	Rotation
3	0.231	4.47	3.23	7.87	13.23	1.68	0.172	4.65	3.08	8.43	14.09	1.67	Simple	Irregular Changes
4	0.152	1.24	2.1	2.76	5.63	2.04	0.112	1.36	2.14	2.3	6.23	2.71	Double	Extension and Rotation
5	0.214	1.79	2.87	2.94	6.39	2.17	0.171	2.05	2.57	2.49	7.51	3.02	Double	Rotation and Expansion
6	0.218	0.36	1.82	3.53	4.05	1.15	0.173	0.56	1.45	2.36	5.12	2.17	Simple	Translation
7	0.196	0.51	1.56	2.46	3.25	1.32	0.174	0.57	1.26	1.41	4.37	3.10	Double	Translation and Rotation
8	0.190	1.92	2.1	3.3	7.45	2.26	0.188	1.65	2.21	3.7	6.74	1.82	Simple	Irregular Changes
9	0.179	2.57	1.58	5.38	9.56	1.78	0.212	1.11	2.42	3.32	5.18	1.56	Cutoff	Cutoff and Redevelopment
10	0.187	1.95	1.4	3.84	11.76	3.06	0.243	0.66	4.17	3.46	4.97	1.44	Cutoff	Cutoff and Redevelopment
11	0.168	0.41	0.86	2.56	3.48	1.36	0.154	1.16	1.1	2.81	3.70	1.32	Cutoff	Cutoff and Redevelopment
12	0.185	0.45	1.15	1.82	3.45	1.90	0.215	0.44	1.83	1.17	3.51	3	Simple	Lateral Movement (Left)
13	0.171	0.75	1.37	1.78	3.58	2.01	0.138	0.69	1.23	1.69	3.85	2.28	Simple	Expansion (Decrease)
14	0.141	0.69	1.15	2.73	3.03	1.40	0.173	0.62	1.01	2.83	3.65	1.29	Simple	Expansion (Decrease)
15	0.248	0.61	1.36	3.66	5.01	1.37	201	0.86	1.34	3.61	4.79	1.33	Double	Extension and Expansion
16	0.175	0.89	1.82	3.52	5.30	1.51	0.168	1.01	1.71	3.42	5.48	1.60	Simple	Expansion (Increase)
17	0.132	0.78	1.45	3.24	4.94	1.52	0.097	0.94	1.54	2.75	4.85	1.76	Simple	Expansion (Increase)
18	0.200	0.50	1.13	3.2	3.81	1.19	0.158	0.63	0.94	2.75	4.01	1.48	Double	Extension and Expansion
19	0.268	0.86	2.56	2.93	5.30	1.81	0.253	0.93	2.05	3.16	4.22	1.97	Simple	Expansion (Decrease)
20	0.172	1.80	2.60	4.59	7.39	1.61	0.170	2.1	2.22	4.7	8.06	1.71	Triple	Extension, Translation and Rotation
Mean	0.194	1.28	1.97	3.65	5.91	1.73	0.176	1.25	2.07	3.35	5.96	1.94		
Min	0.132	0.36	0.86	1.78	3.03	1.15	0.097	0.44	0.94	1.17	3.51	1.29		
Max	0.268	4.47	4.13	7.87	13.23	3.06	0.253	4.65	4.17	8.43	14.09	3.10		
SD	0.0367	0.99	0.87	1.46	2.92	0.45	0.0376	0.94	0.94	1.64	2.67	0.59		

726
727
728
729
730
731
732

733

Table 6

734

Results of paired sample *T*-test for the parameters of the meanders between two dates (1989 and 2008)

735

Meander parameter	Average difference between variables	Standard deviation	T value	Degree of freedom	Sig.
L	0.2957	0.6144	2.152	19	0.044*
S	0.2385	1.9336	0.552	19	0.588
W	19.9	36.201	2.458	19	0.024*
C	-0.2105	0.6827	-1.379	19	0.184
R	0.0245	0.5075	0.216	19	0.831
A	0.097	0.7108	0.610	19	0.549

736

* Significant at 5% confidence level.

737

738

739

740

741

742

743

744

745

746

747

748

749

750

751

752

753

754

755
756
757
758

Table 7

Results of the Pearson correlation between meander parameter changes between 1989 and 2008

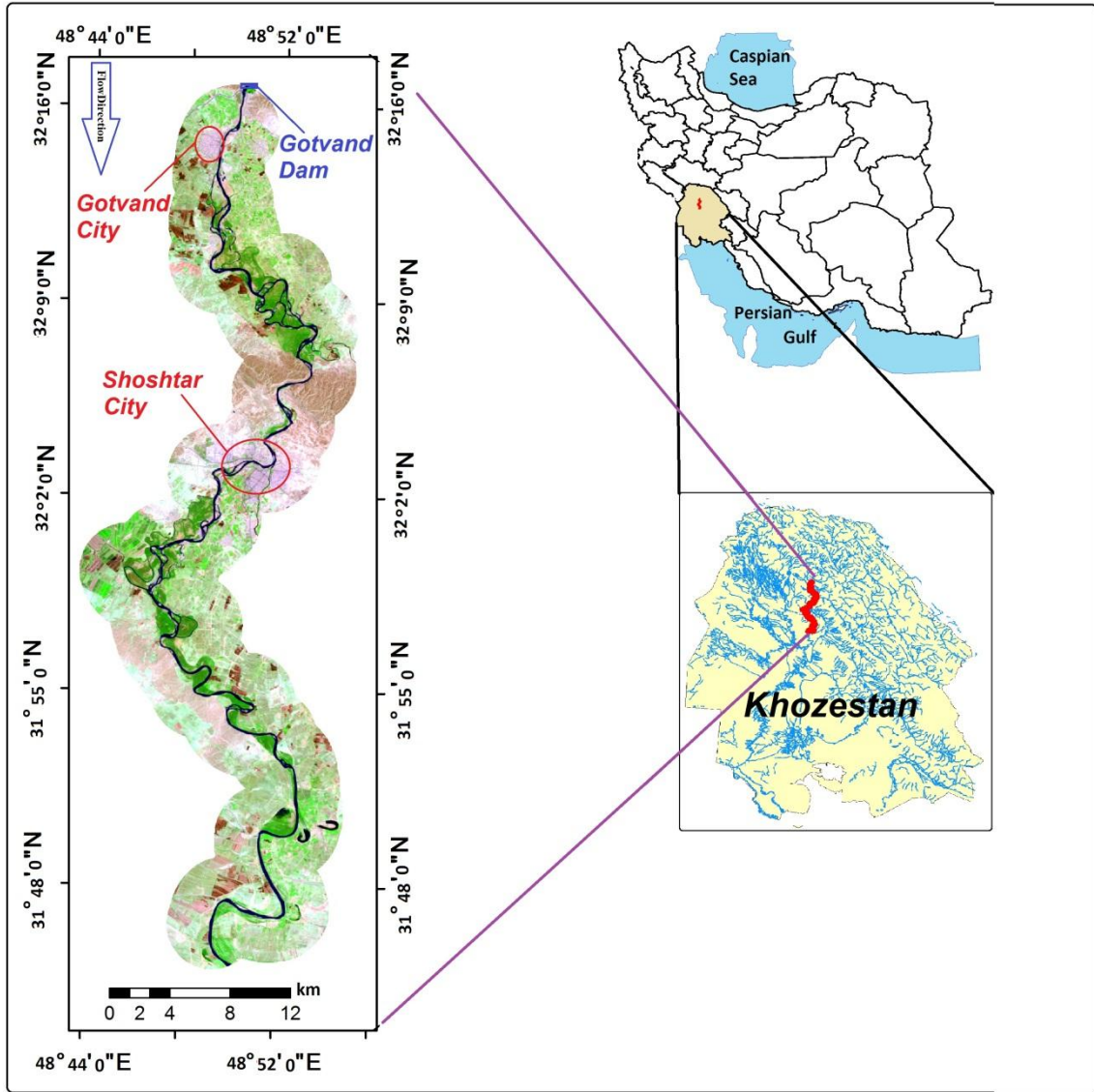
Meander parameter	Statistical factor	C	R	W	L	S	A
C	r ¹	a					
	Sig.						
R	r	0.510*	a				
	Sig.	0.022					
W	r	-0.367	-0.605**	a			
	Sig.	0.111	0.005				
L	r	-0.329	0.479*	-0.219	a		
	Sig.	0.156	0.033	0.353			
S	r	0.725**	0.881**	-0.648**	0.327	a	
	Sig.	0.000	0.000	0.002	0.159		
A	r	0.624**	0.730**	0.641**	0.219	0.919**	a
	Sig.	0.003	0.000	0.002	0.354	0.000	

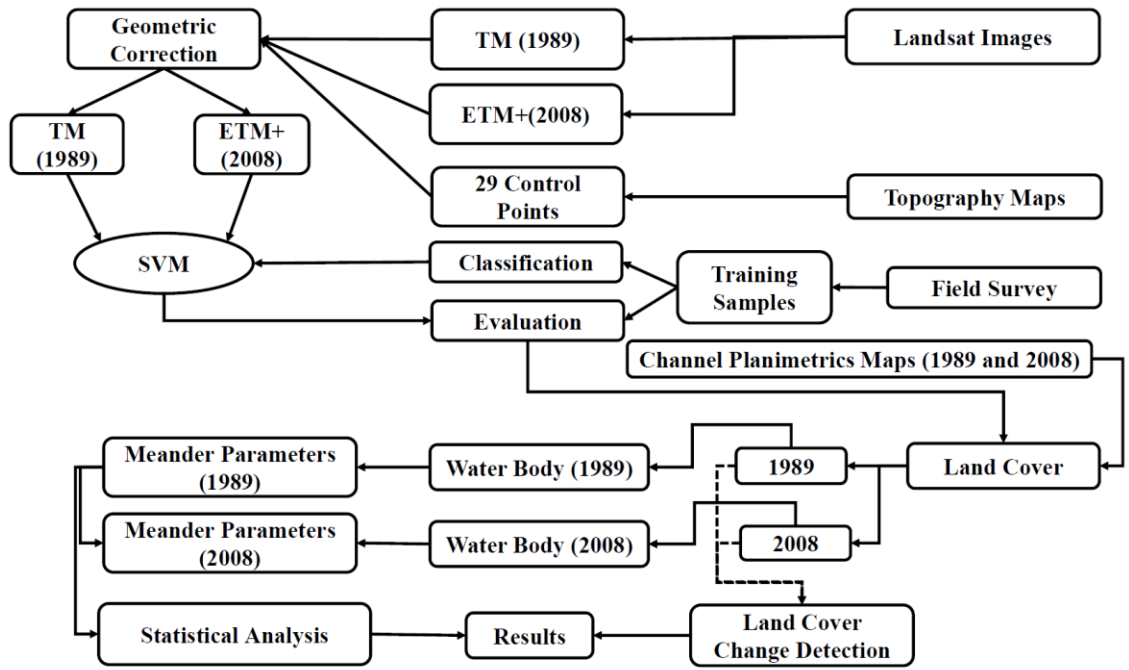
759
760
761

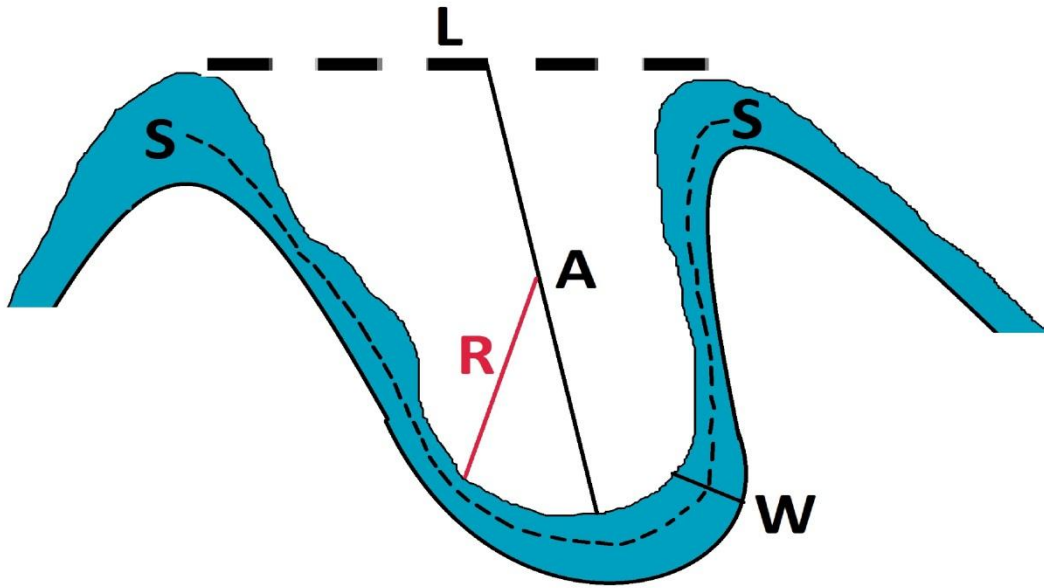
* Significant at 5% confidence level.

** Significant at 1% confidence level.

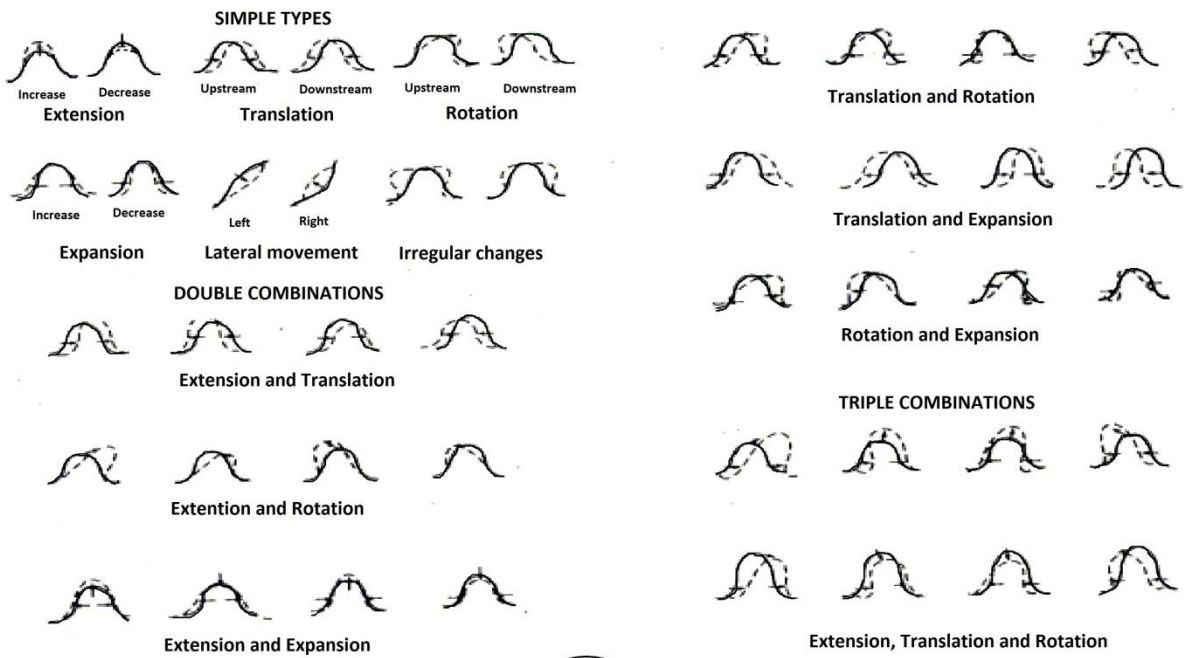
¹Pearson correlation coefficient.





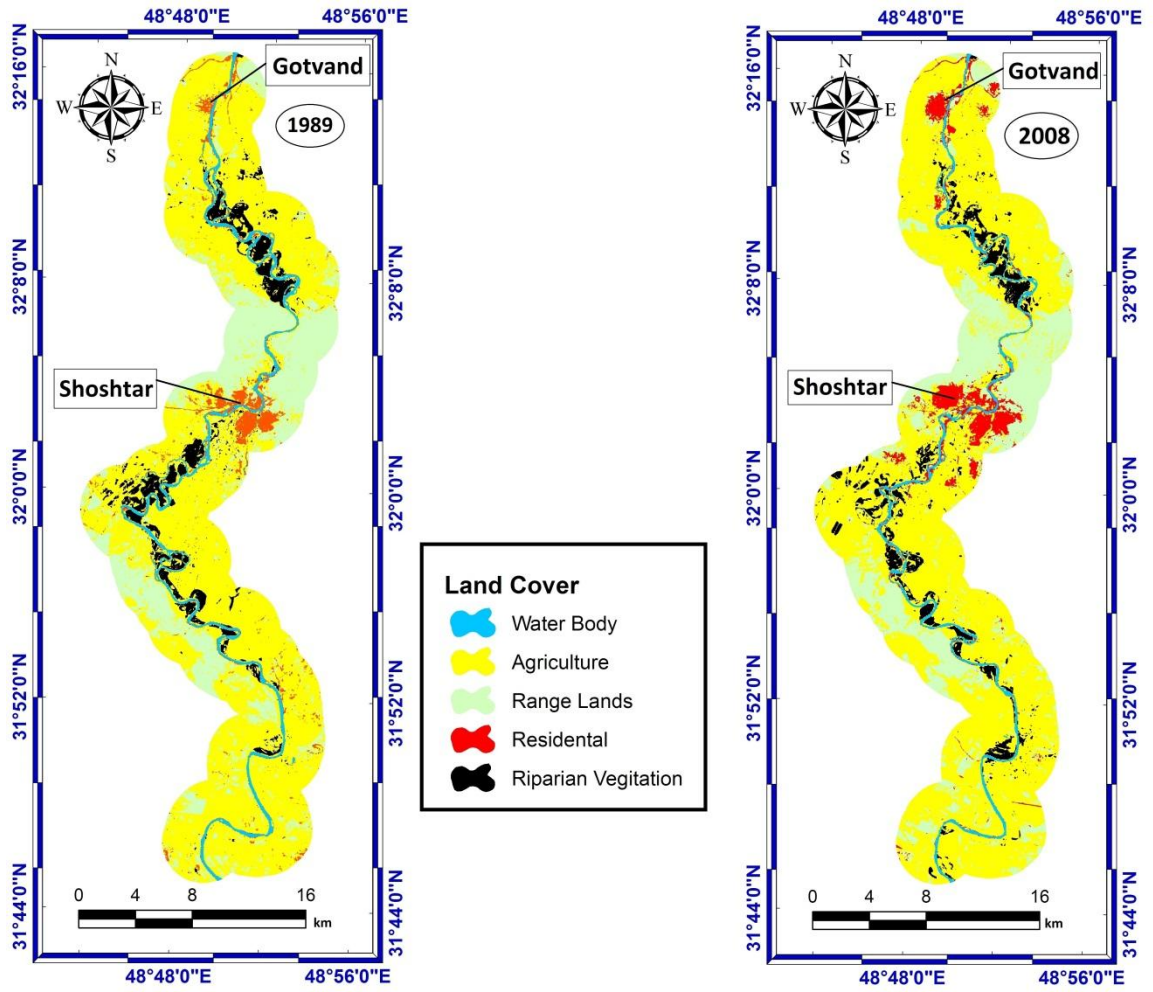


A



B

767



768

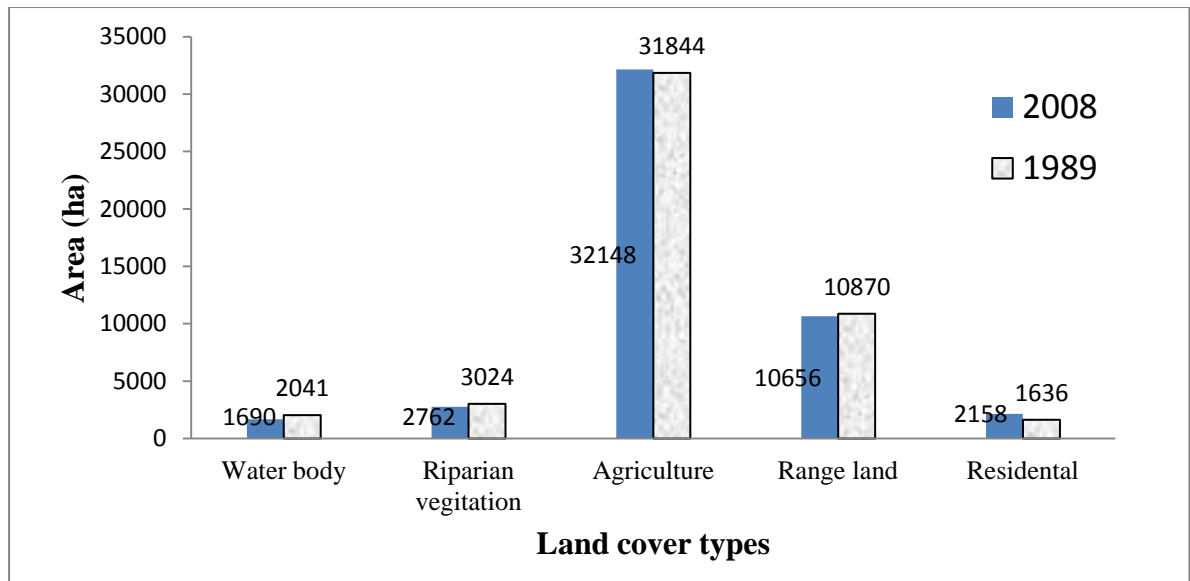
769

770

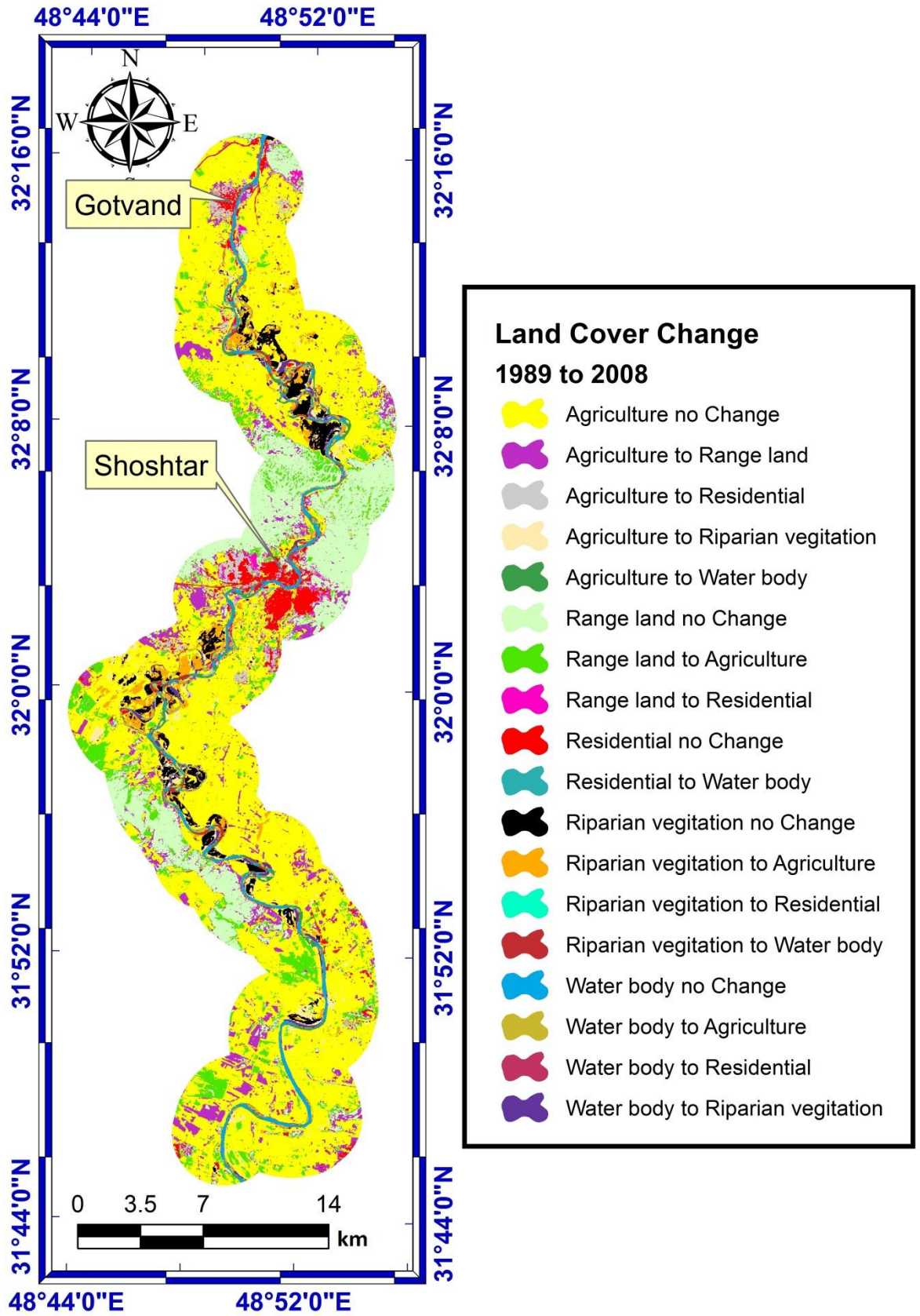
771

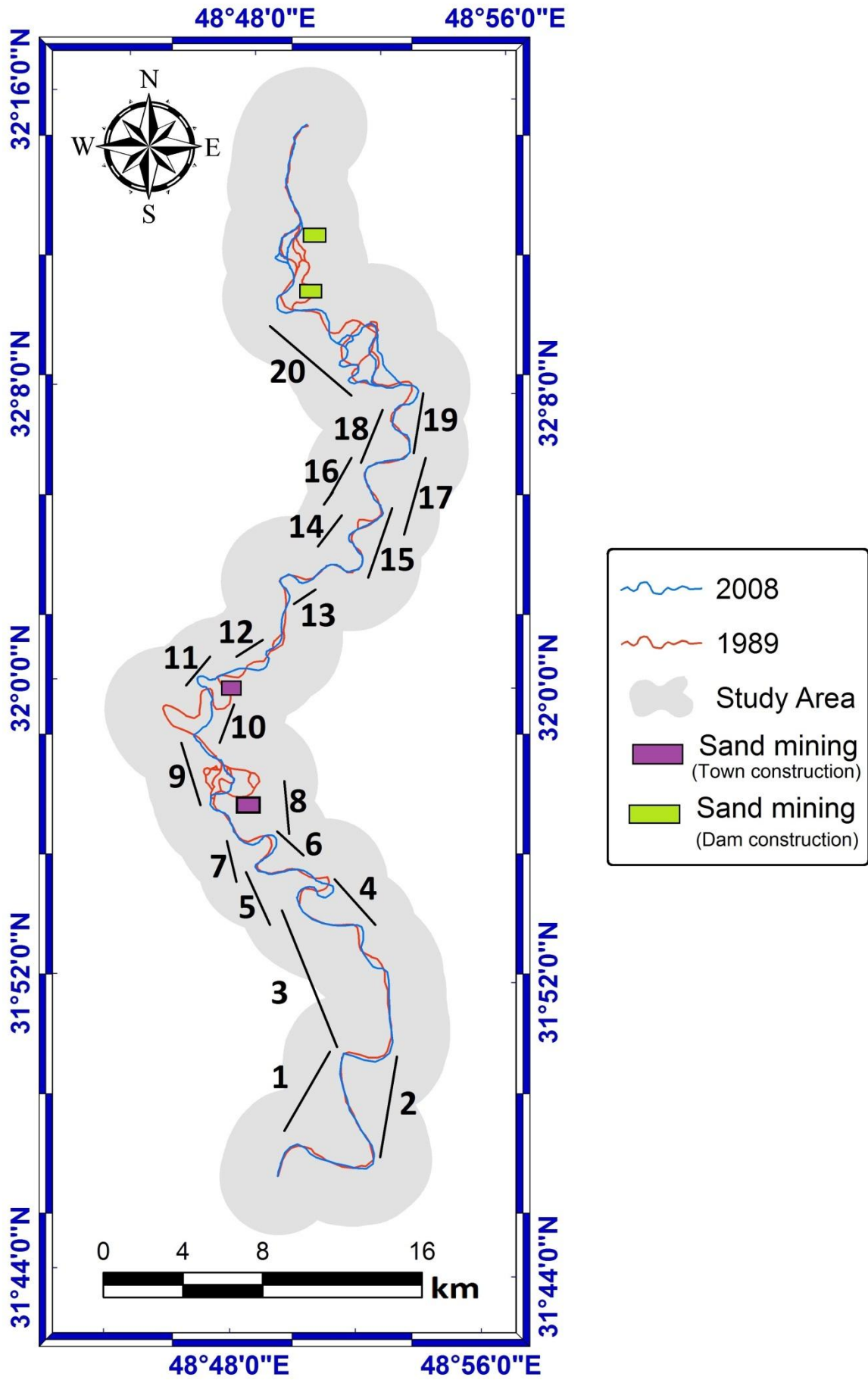
772

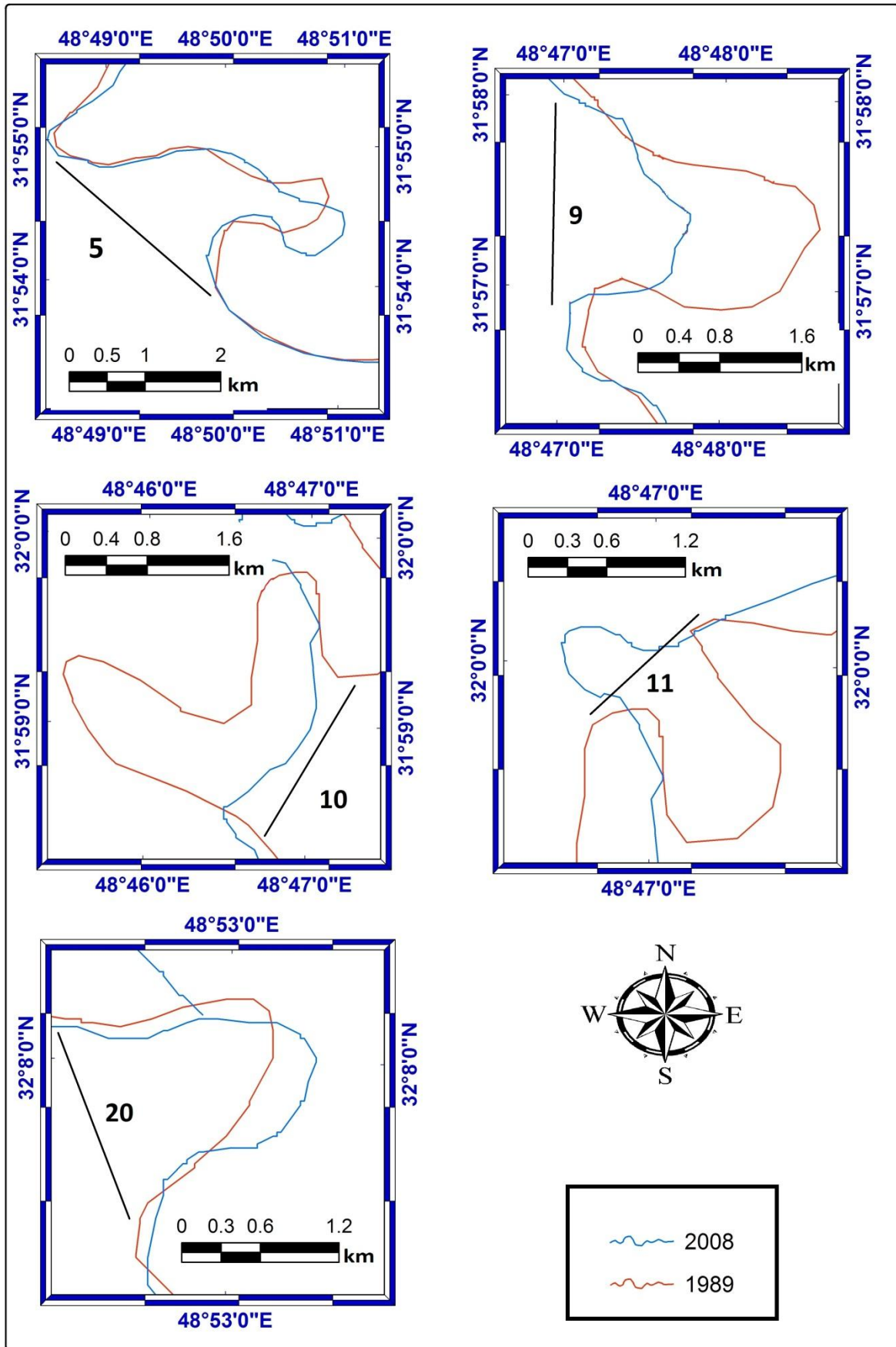
773

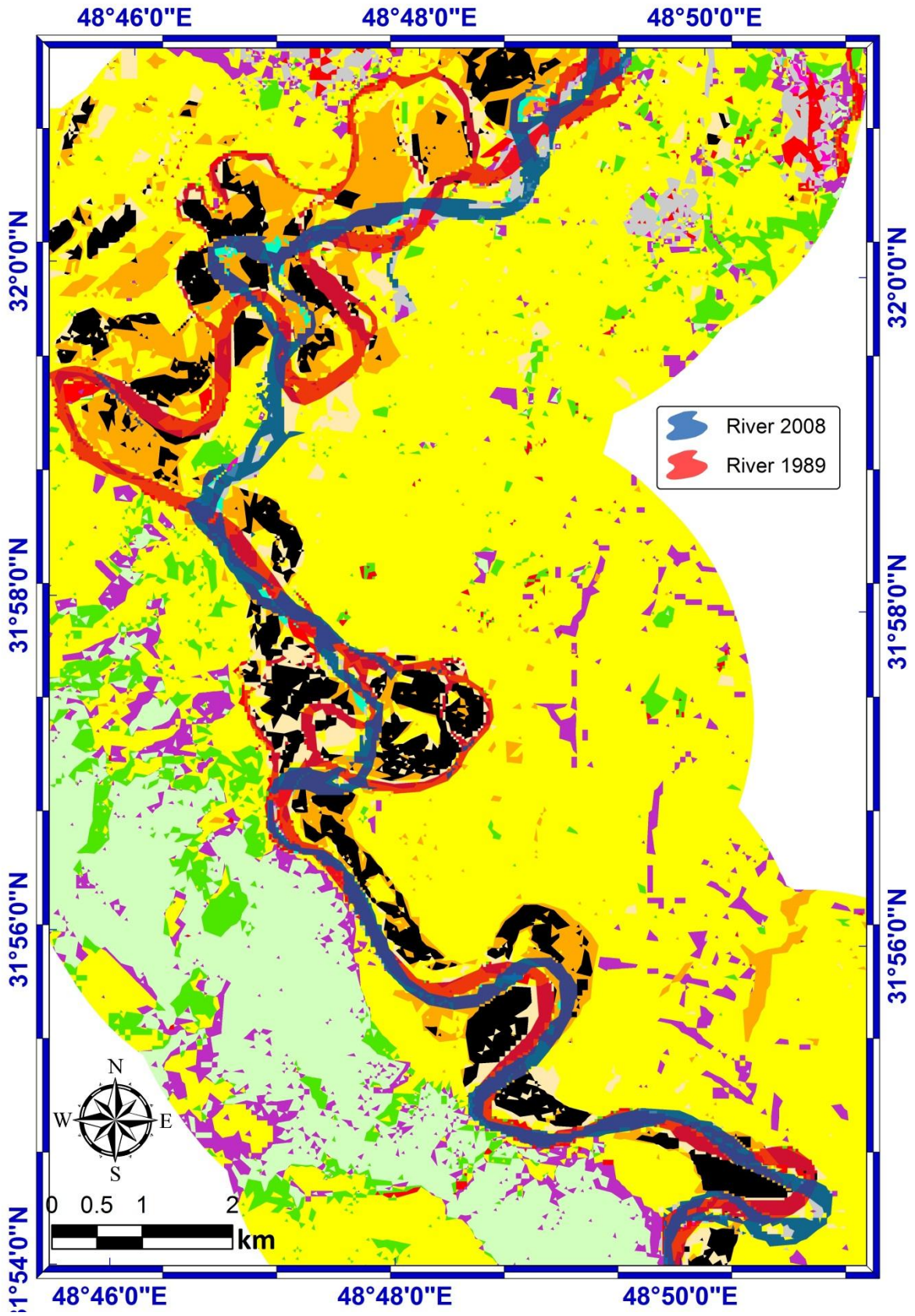


774









778
779